Chobeau, Pierre; Savioja, Lauri

Memory cost of absorbing conditions for the finite-difference time-domain method

Published in:
Journal of the Acoustical Society of America

DOI:
10.1121/1.4958977

Published: 01/07/2016

Document Version
Publisher's PDF, also known as Version of record

Please cite the original version:
Chobeau, P., & Savioja, L. (2016). Memory cost of absorbing conditions for the finite-difference time-domain method. *Journal of the Acoustical Society of America*, *140*(1), EL119-EL124. https://doi.org/10.1121/1.4958977

Memory cost of absorbing conditions for the finite-difference time-domain method

Pierre Chobeau and Lauri Savioja
Department of Computer Science, Aalto University, Otaniementie 17, FI-02150 Espoo, Finland
pierre.chobeau@aalto.fi, lauri.savioja@aalto.fi

Abstract: Three absorbing layers are investigated using standard rectilinear finite-difference schemes. The perfectly matched layer (PML) is compared with basic lossy layers terminated by two types of absorbing boundary conditions, all simulated using equivalent memory consumption. Lossy layers present the advantage of being scalar schemes, whereas the PML relies on a staggered scheme where both velocity and pressure are split. Although the PML gives the lowest reflection magnitudes over all frequencies and incidence angles, the most efficient lossy layer gives reflection magnitudes of the same order as the PML from mid- to high-frequency and for restricted incidence angles.

[CFG]
Date Received: January 19, 2016 **Date Accepted:** May 10, 2016

1. Introduction

Simulations of free-field condition using a truncated numerical domain require a truncation that shows both significant absorption of outgoing waves and a low memory consumption. The numerical techniques used for the domain truncation can be split into two categories: absorbing boundary conditions and absorbing layers. Whereas absorbing boundary conditions are usually applied on a single node, absorbing layers are defined over the range of nodes constituting the layer thickness. Although absorbing conditions have been tested under various types of configuration with time-domain methods, their efficiency is not often related to their relative memory requirements.

Modern finite-difference time-domain (FDTD) simulations are often computed on massively parallel computation hardware such as graphics processing units (GPUs).[1] In those environments, the computational performance is typically limited by the memory bandwidth as opposed to being compute-bound. For this reason, our main focus is on memory usage although numbers of required operations are reported as well. The selected absorbing techniques are tested for equivalent memory consumption using standard rectilinear- (SRL-) FDTD updates, also known as standard leapfrog.[2] The numerical results, simulated using two-dimensional (2D) domains, give an estimate of the absorbing efficiency as a function of frequency, incidence angle and layer thickness. The theory related to absorbing conditions is briefly reviewed in Sec. 2. The numerical results are presented in Sec. 3.

2. Theory

2.1 Absorbing boundary conditions

In this section, a 2D Cartesian coordinate system (x, y) is considered. The boundary is parallel to the y-axis, and perpendicular to the propagation direction that follows the x-axis.

The first-order Engquist and Majda boundary condition[3] (EM-BC) at $x = x_{(b)}$ is given by

$$\frac{\partial p}{\partial x_{(b)}} - \frac{1}{c}\frac{\partial p}{\partial t} = 0, \tag{1}$$

where c is the sound speed. Equation (1) can be written as a two-step (in time) SRL-FDTD update

$$\widehat{p}_i^{n+1} = \left[1 + \frac{N_{(b)}\lambda}{2}\right]^{-1} \left(\lambda^2 \left(\sum_{j=1}^{N-N_{(b)}} \widehat{p}_j^n - \left(N - N_{(b)}\right)\widehat{p}_i^n \right) + 2\widehat{p}_i^n - \left[1 + \frac{N_{(b)}\lambda}{2}\right]\widehat{p}_i^{n-1} \right), \tag{2}$$

where $\widehat{p}_i^n$ is the discretized pressure at the node i and at the discrete time n, j corresponds to the axial nodes, N is the total number of axial nodes, $N_{(b)}$ is an indicator function giving the number of boundary nodes, and λ is the Courant number defined by

$$\lambda = \frac{cT_s}{h}, \tag{3}$$

where T_s is the time step and h is the spatial step.

The second-order Taylor series (T-BC) defined for the digital waveguide method[4] can be applied to numerical methods that use rectilinear topologies such as the SRL-FDTD method. The T-BC is defined as follows:

$$\widehat{p}_{i(b)}^{n+1} = \frac{5}{2}\widehat{p}_{i(b)-1}^{n} - 2\widehat{p}_{i(b)-2}^{n-1} + \frac{1}{2}\widehat{p}_{i(b)-3}^{n-2}, \tag{4}$$

where the subscript $i(b)$ corresponds to the location of the boundary. Compared to EM-BC, it requires an additional step: $\widehat{p}_{i(b)-3}^{n-2}$. The SRL-FDTD update form of the T-BC is a three-step scheme written as

$$\begin{aligned}\widehat{p}_i^{n+1} = {} & \lambda^2\left(\sum_{j=1}^{N-N_{(b)}}\widehat{p}_j^n - \left(N - N_{(b)}\right)\widehat{p}_i^n\right) + 2\widehat{p}_i^n - \widehat{p}_i^{n-1} \\ & + N_{(b)}\left(\frac{5}{2}\widehat{p}_{i(b)-1}^{n} - 2\widehat{p}_{i(b)-2}^{n-1} + \frac{1}{2}\widehat{p}_{i(b)-3}^{n-2}\right).\end{aligned} \tag{5}$$

2.2 Absorbing layers

An absorbing layer can be seen as an anisotropic media that gradually decreases the pressure field magnitude along a given direction.

The basic lossy layer (LL) can be derived from the lossy wave equation

$$\frac{\partial^2 p}{\partial t^2} - c^2\Delta p + 2\sigma\frac{\partial p}{\partial t} = 0, \tag{6}$$

where σ is the attenuation factor that gradually increases following the main propagation direction inside the absorbing layer, i.e., the direction normal to the boundary. It is defined as

$$\sigma_x = \sigma_{\max}\left(\frac{x - x_0}{e_{\mathrm{AL}}}\right)^2, \tag{7}$$

where e_{AL} is the layer thickness, x_0 the beginning of the absorbing layer, $x \in [x_0, x_{e_{\mathrm{AL}}}]$. The attenuation factor is equal to zero outside the absorbing layer. The value of $\sigma_{\max}$ in Eq. (7) is empirically determined for given layer thickness by minimizing both the round-trip and the transition reflections.[5] The quadratic shape is chosen as a compromise between linear and higher orders shape to minimize the transition reflection and increase the performance of the layer.[6] The SRL-FDTD update for Eq. (6) can be written

$$\widehat{p}_i^{n+1} = [1 + \sigma T_s]^{-1}\left(\lambda^2\left(\sum_{j=1}^{N}\widehat{p}_j^n - N\widehat{p}_i^n\right) + 2\widehat{p}_i^n - [1 - \sigma T_s]\widehat{p}_i^{n-1}\right). \tag{8}$$

The perfectly matched layer (PML) can be defined using different approaches as reminded by Osokoi *et al.*[5] It is chosen here to use a staggered finite difference scheme,[8] where the velocity and pressure grids are interleaved in both space and time. In 2D, the update can be written as[7]

$$\widehat{v}_{x\,i,j}^{\,n+0.5} = e_x^{\zeta}\widehat{v}_{x\,i,j}^{\,n-0.5} - e_x^{\gamma}(\widehat{p}_{x\,i+1,j}^{\,n} - \widehat{p}_{x\,i,j}^{\,n}), \tag{9a}$$

$$\widehat{v}_{y\,i,j}^{\,n+0.5} = e_y^{\zeta}\widehat{v}_{y\,i,j}^{\,n-0.5} - e_y^{\gamma}(\widehat{p}_{y\,i,j+1}^{\,n} - \widehat{p}_{y\,i,j}^{\,n}), \tag{9b}$$

followed by the pressure update

$$\widehat{p}_{x\,i,j}^{\,n+1} = e_x^{\alpha}\widehat{p}_{i,j}^{n} - e_x^{\beta}(\widehat{v}_{x\,i,j}^{\,n+0.5} - \widehat{v}_{x\,i-1,j}^{\,n+0.5}), \tag{10a}$$

$$\widehat{p}_{y\,i,j}^{\,n+1} = e_y^{\alpha}\widehat{p}_{i,j}^{n} - e_y^{\beta}(\widehat{v}_{y\,i,j}^{\,n+0.5} - \widehat{v}_{y\,i,j-1}^{\,n+0.5}), \tag{10b}$$

where $\widehat{p}_{i,j}^{n+1} = \widehat{p}_{x\,i,j}^{\,n+1} + \widehat{p}_{y\,i,j}^{\,n+1}$. The factors e^{α}, e^{β}, e^{ζ}, and e^{γ} are defined for the x coordinate as

Table 1. Memory requirements for each absorbing condition for a layer thickness of N pressure-nodes, n_{dim} dimensional space, and $n_{\sigma\mathrm{dir}}$ the number of attenuation factor directions.

	EM-BC	T-BC	LL	PML
Thickness (pressure-node)	1	1	N	N
Additions	$5+n_{\mathrm{dim}}$	$6+2n_{\mathrm{dim}}$	$5+2n_{\mathrm{dim}}$	$4n_{\mathrm{dim}}+(n_{\mathrm{dim}}-1)$
Multiplications	9	7	7	$4n_{\mathrm{dim}}$
Total operations per pressure-node	$14+2n_{\mathrm{dim}}$	$13+2n_{\mathrm{dim}}$	$N(12+2n_{\mathrm{dim}})$	$N(8n_{\mathrm{dim}}+(n_{\mathrm{dim}}-1))$
Memory consumption (stored values)	3	4	$N(2+n_{\sigma\mathrm{dir}})$	$N(2n_{\mathrm{dim}}+4n_{\sigma\mathrm{dir}})$

$$e_x^{\alpha} = e^{-\sigma_x T_s \rho c^2}, \quad e_x^{\beta} = \frac{1-e^{-\sigma_x T_s \rho c^2}}{h\sigma_x}, \tag{11a}$$

$$e_x^{\zeta} = e^{-\sigma_x T_s}, \quad e_x^{\gamma} = \frac{1-e^{-\sigma_x T_s}}{h\rho\sigma_x}. \tag{11b}$$

Equations (11) for y and z coordinates follow a similar form and are not given here for brevity. The attenuation factor σ_x is defined following Eq. (7), and the maximum value is set using[7]

$$\sigma_{\mathrm{max-PML}} = -\frac{\log R}{\rho c h}, \tag{12}$$

where the value of the reflection coefficient R is set to be at the lowest and adjusted by minimizing the round-trip and the transition reflections[5] for the average layer thickness.

2.3 Memory requirements

The number of operations and the memory consumption per pressure-node is given in Table 1 for n_{dim} dimensional space. The thickness of the layer N and the number of attenuation directions $n_{\sigma\mathrm{dir}}$ are taken into account in the estimation of the final memory consumption of each layer. Both boundary conditions EM-BC and T-BC present similar memory consumption. The PML, because of the staggered scheme and the split pressure field in Eqs. (9) and (10), presents a larger memory cost than the LL. For instance, a 2D ($n_{\mathrm{dim}}=2$) and single direction ($n_{\sigma\mathrm{dir}}=1$) PML of $N=4$ pressure-node thickness is equivalent in memory to a 10 nodes LL (Sec. 3.2).

3. Numerical results

Both boundaries and layers can be numerically tested by taking advantage of the geometrical symmetry that allows to reduce the dimension of the domain from 3D to 2D, without loss of information. The following simulations are implemented using 2D schemes, which still enables to test several incidence angles and layer thicknesses.

3.1 Simulation settings and principle

The numerical domain used for 2D simulations is made of a propagation domain and an absorbing condition, as depicted in Fig. 1. The source and the receivers are located at the same distance from the absorbing boundary or from the entrance of the absorbing layer.

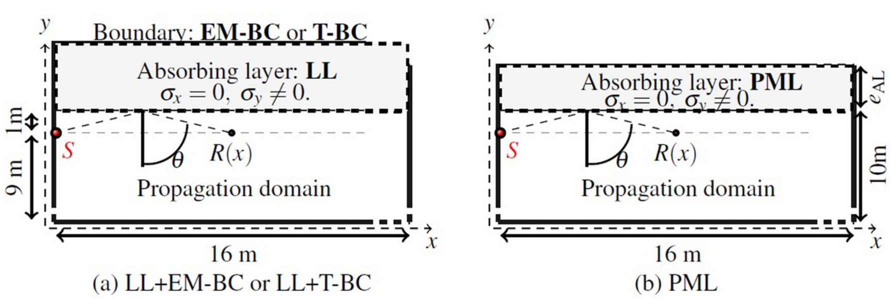

Fig. 1. (Color online) Computational domain (2D) used for the assessment of the efficiency of (a) the combination of LL+ EM-BC or LL+T-BC; (b) PML.

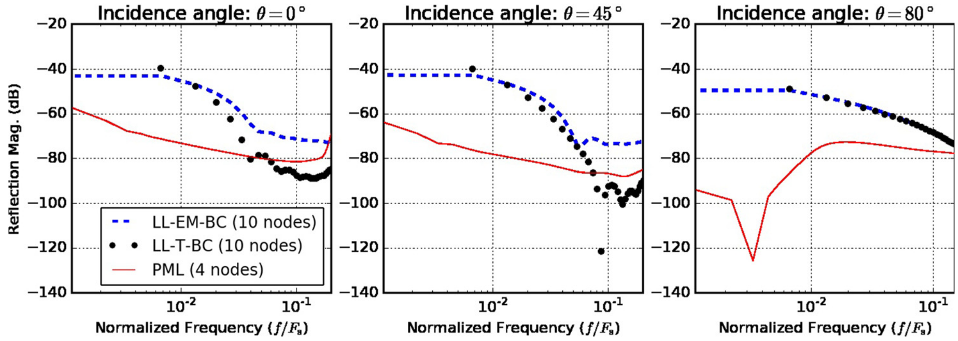

Fig. 2. (Color online) Reflection magnitude (dB) obtained with the LL-EM-BC, the LL-T-BC, and the PML, for three angles of incidence 0°, 45°, and 80°.

Eighty-one receivers are located along a line parallel to the boundary or the layer at distances that correspond to angle of incidence θ ranging from 0° to 80°.

The propagation domain is made of a scalar pressure scheme computed over a grid of regularly spaced pressure-nodes. The PML is the only absorbing condition that requires interleaved pressure and velocity grids,[8] i.e., the scheme is staggered. In this case, SRL scalar and staggered schemes are equivalent[9] and can be directly connected to each other.

The sampling frequency is set equal to $F_s = 8000$ Hz, which is equivalent to a time step $T_s = 1.25 = 10^{-4}$ s. The simulations are carried out at the Courant limit $\lambda = 1/\sqrt{2}$. Using a sound speed $c = 340\,\mathrm{m\,s^{-1}}$ gives a spatial step equal to $h = 6.00 \times 10^{-2}$ m. The total number of time steps for a simulation is set equal to 448, i.e., 0.056 s. The source is soft type[10] that emits a pulse with a constant frequency content in the range $f = [0, 2000]$ Hz, that corresponds to a normalized frequency range of $f_{\mathrm{norm}} = f/F_s = [0, 0.25]$.

The thicknesses of the studied layers are constricted in $e_{\mathrm{AL}} = [4\text{–}32]$ pressure-nodes $\sim[0.24\text{–}1.92]$ m. The maximum value of the lossy layer attenuation factor is empirically set[5] at $\sigma_{\max} = 3000\,\mathrm{s^{-1}}$. In the case of the PML,[7] $\sigma_{\max\text{–PML}} = 0.18\,\mathrm{s^{-1}}$ that corresponds to a reflection coefficient $R = 0.01$ in Eq. (12).

The reflection magnitude is calculated in two steps: first, the free-field pressure $\hat{p}_{\mathrm{free}}$ is calculated using an extended propagation domain where outgoing waves do not collide with any boundary during the simulation duration. Second, the acoustic pressure $\hat{p}$ is calculated at the same location in presence of absorbing conditions. The acoustic pressures $\hat{p}$ and $\hat{p}_{\mathrm{free}}$ are windowed and transformed in the frequency-domain that gives $\tilde{P}$ and $\tilde{P}_{\mathrm{free}}$, respectively. The absolute value of the difference between the two frequency-variables gives the reflection magnitude as a function of frequency. This reflection magnitude is presented in dB as

$$\mathrm{R}(f) = 20\log_{10}(|\tilde{P}_{\mathrm{free}} - \tilde{P}|). \tag{13}$$

3.2 Preliminary observations on the absorbing conditions

The basic LL, because of its simplistic approach, presents only poor absorbing properties compared with the PML that has already proved to be a highly absorbing layer.[7]

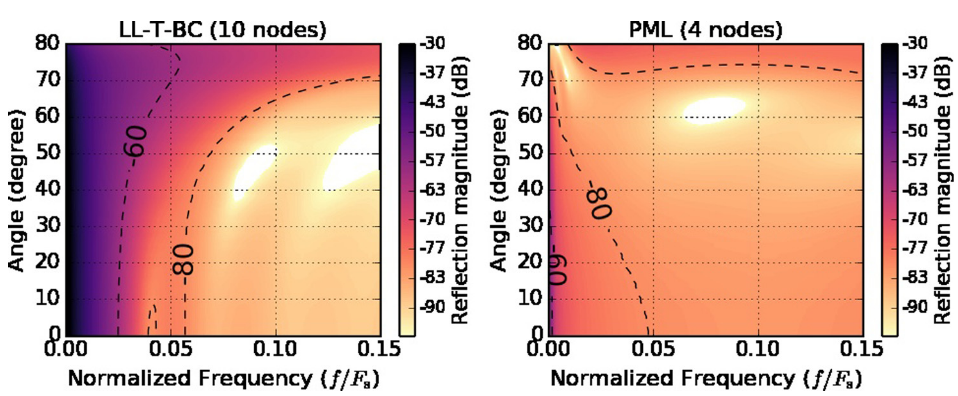

Fig. 3. (Color online) Reflection magnitude in dB for incidence angles ranging from 0° to 80° along frequency for the LL-T-BC (left) and the PML (right).

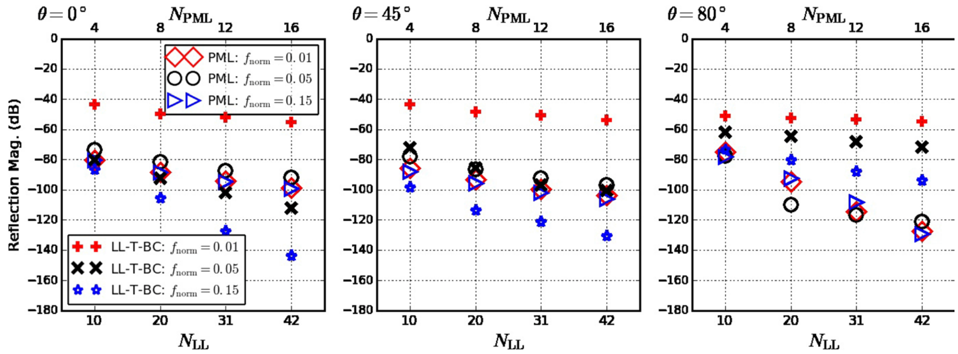

Fig. 4. (Color online) Reflection magnitude (dB) as a function of layer thicknesses (number of pressure-node) N_{PML} and N_{LL} taken for equal memory cost between the PML and the LL-T-BC, for three angles of incidence $\theta = 0°$ (left), $\theta = 45°$ (middle), and $\theta = 80°$ (right).

However, absorbing properties of the LL can be improved using an absorbing termination such as the EM-BC or the T-BC [Fig. 1(a)], which gives two layers: the LL-EM-BC and the LL-T-BC, respectively. The following numerical results focus on the reflection magnitude given by the three absorbing layers: the LL-EM-BC, the LL-T-BC, and the PML, all for equal memory consumption.

Considering a 2D ($n_{\mathrm{dim}} = 2$) and single direction ($n_{\sigma\mathrm{dir}} = 1$) PML of N_{PML} pressure-nodes, the equivalence between N_{PML} and N_{LL} for equal memory consumption is given by $8N_{\mathrm{PML}} = 3N_{\mathrm{LL}} + 3N_{\mathrm{EM\text{-}BC}} = 3N_{\mathrm{LL}} + 4N_{\mathrm{T\text{-}BC}}$, where $N_{\mathrm{EM\text{-}BC}} = N_{\mathrm{T\text{-}BC}} = 1$. Averaging the number of nodes N_{LL} between the LL-EM-BC and the LL-T-BC, for a range of $N_{\mathrm{PML}} = [4, 8, 12, 16]$ nodes, gives a unique equivalent set of $N_{\mathrm{LL}} = [10, 20, 31, 42]$ nodes.

3.3 Results

The reflection magnitudes obtained with the three layers LL-EM-BC, LL-T-BC, and PML, are shown in Fig. 2, at three incidence angles and for equal memory consumption. Among the three layers, the LL-EM-BC presents the highest reflection magnitudes. Although the LL-T-BC presents for specific frequencies the lowest reflection, the PML remains on average overall frequencies and angles the most absorbing layer as shown in Fig. 3.

Four layer thicknesses are compared in Fig. 4 between the LL-T-BC and the PML for three incidence angles and three frequencies, i.e., $f_{\mathrm{norm}} = 0.01$, 0.05, and 0.15. The LL-T-BC presents lower reflection magnitudes than the PML at 0° and 45° only at the highest frequency. For larger incidence angles the PML remains the most absorbing layer.

4. Conclusions

Three absorbing layers have been compared to each other using the SRL-FDTD schemes of equivalent memory consumption. The PML and the LL-T-BC present the lowest reflection magnitudes. The PML performs better than the LL-T-BC at low frequencies for all incidence angles, and for large incidence angles at all frequencies. The LL-T-BC gives similar or better performance than the PML at mid- and high-frequencies for low incidence angles. In terms of memory, the PML is the only approach that requires a staggered pressure and velocity scheme, where the pressure field is split following each direction. In comparison, the LL-T-BC only requires a scalar pressure grid and an additional stored value at the boundary. Considering both the absorbing efficiency and the memory cost, for specific geometries where low incidence angles are predominant, the LL-T-BC can be an alternative absorbing scheme of interest.

Acknowledgments

This work has received funding from Academy of Finland, Project No. 265824.

References and links

[1] L. Savioja, "Real-time 3D finite-difference time-domain simulation of low- and mid-frequency room acoustics," in *Proceedings of Digital Audio Effects 2010 (DAFx-10)* (2010).

[2] K. Kowalczyk and M. van Walstijn, "Room acoustics simulation using 3-D compact explicit FDTD schemes," IEEE Trans. Audio Speech Lang. Process. **19**, 34–46 (2011).

[3] B. Engquist and A. Majda, "Absorbing boundary conditions for the numerical simulation of waves Mathematics of Computation," Math. Comput. **31**, 629–651 (1977).

[4]Z. Ghen, M. Ney, and W. Hoefer, "Absorbing and connecting boundary conditions for the TLM method," IEEE Trans. Microwave Theory Tech. **41**, 2016–2024 (1993).
[5]A. Oskooi and S. G. Johnson, "Distinguishing correct from incorrect PML proposals and a corrected unsplit PML for anisotropic, dispersive media," J. Comput. Phys. **230**, 2369–2377 (2011).
[6]P. Mokhtari, H. Takemoto, R. Nishimura, and H. Kato, "Optimum loss factor for a perfectly matched layer in finite-difference time-domain acoustic simulation," IEEE Trans. Audio Speech Lang. Process. **18**, 1068–1071 (2010).
[7]X. Yuan, D. Borup, J. Wiskin, M. Berggren, R. Eidens, and S. Johnson, "Formulation and validation of Berenger's PML absorbing boundary for the FDTD simulation of acoustic scattering," IEEE Trans. Ultrason. Ferroelectr. Freq. Control **44**, 816–822 (1997).
[8]K. Yee, "Numerical solution of initial boundary value problems involving Maxwell's equations in isotropic media," IEEE Trans. Ant. Propag. **14**, 302–307 (1966).
[9]J. Botts and L. Savioja, "Integrating finite difference schemes for scalar and vector wave equations," in *2013 IEEE International Conference on Acoustics, Speech and Signal Processing* (2013).
[10]A. Taflove and S. C. Hagness, *Computational Electrodynamics: The Finite-Difference Time-Domain Method* (Artech House, London, 2000).